CHEMISTRY OF MATERIALS
Article

Chem. Mater. **2010,** *22,* 1195–1202 1195
DOI:10.1021/cm902685m

Enhancement of Electrochemical Performance of Macroporous Carbon by Surface Coating of Polyaniline†

Li Li Zhang,‡ Shi Li,§ Jintao Zhang,‡ Peizhi Guo,⊥ Jingtang Zheng,∥ and X. S. Zhao*,‡,⊥

‡*Department of Chemical and Biomolecular Engineering, National University of Singapore, 4 Engineering Drive 4, Singapore 117576,* §*Department of Environmental Science and Engineering, China University of Petroleum, P. R. China,* ⊥*Institute of Multifunctional Materials (IMM), Laboratory of New Fiber Materials and Modern Textile, The Growing Base for State Key Laboratory, Qingdao University, Qingdao 266071, P. R. China, and* ∥*State Key Laboratory of Heavy Oil Processing, China University of Petroleum, Dongying 257061, P. R. China*

Received August 31, 2009. Revised Manuscript Received November 6, 2009

Conducting polymer-macroporous carbon composite electrode materials were prepared by deposition of a thin layer of polyaniline (PANI) on the surface of three-dimensionally ordered macroporous carbon. A specific capacitance of 1490 F/g was observed over the deposited PANI in the composite electrode. Good rate performance and cycle ability were realized on the composite electrode, attributed to the combined contribution from both the unique properties of the carbon matrix (e.g., highly ordered interconnected pores and good electrical conductivity) and pseudocapacitance of the deposited PANI layer. The three-dimensionally ordered pore structure of the carbon favored the diffusion of the electrolyte ions, hence not only improving the energy storage capacity but also enhancing power density.

Introduction

Supercapacitors attract rapidly growing research interests because of their high power density and long cycle life.[1−4] Two types of mechanisms are associated with energy storage in a supercapacitor, namely electrical double layer (EDL) charge storage and pseudoprocess charge storage.[1] The capacitance of the former comes from the charge accumulation at the electrode/electrolyte interface, and therefore highly dependent on the pore structure of the electrode, such as pore size and accessible surface area to the electrolyte.[5−7] The capacitance of the latter is due to the fast reversible faradic transitions of electro-active species of the electrode, such as surface functional groups,[8] transition metal oxides[9], and conducting polymers.[10] Recent efforts on electrode materials have been devoted to designing advanced materials with well-defined chemical and physical properties to achieve an enhanced energy density (in particular) and a great power density (in general).[2,3]

Activated carbon is the most widely studied electrode material. But the key problem with the activated carbon lies in the slow ion transportation in the small micropores.[11−13] Three-dimensionally ordered macroporous (3DOM) carbons with a hierarchical porous structure can facilitate ion transport, thus displaying great performance as supercapacitor electrodes.[11,14−16] The 3DOM carbons with mesoporous walls have been observed to exhibit an excellent rate capability but with a low energy density.[17] Very recently, three-dimensionally ordered mesoporous carbon sphere arrays have been found to show a good rate performance,[18] but energy storage capacity is lower as compared to the activated carbon. It is obvious that the three-dimensional pore structure with a short diffusion path can indeed provide an ideal pathway for ion transport.

The pseudocapacitance from reversible faradic reactions of an electro-active material affords a higher energy

† Accepted as part of the 2010 "Materials Chemistry of Energy Conversion Special Issue".

*Corresponding author. E-mail: chezxs@nus.edu.sg. Fax: 65-67791936.

(1) Conway, B. E. *Electrochemical Supercapacitors: Scientific Fundamentals and Technological Applications*; Plenum Publisher: New York, 1999.
(2) Simon, P.; Gogotsi, Y. *Nat. Mater.* **2008**, *7*, 845.
(3) Zhang, L. L.; Zhao, X. S. *Chem. Soc. Rev.* **2009**, *38*, 2520.
(4) Miller, J. R.; Simon, P. *Science* **2008**, *32*, 1651.
(5) Fuertes, A. B.; Pico, F.; Rojo, J. M. *J. Power Sources* **2004**, *133*, 329.
(6) Largeot, C.; Portet, C.; Chmiola, J.; Taberna, P. L.; Gogotsi, Y.; Simon, P. *J. Am. Chem. Soc.* **2008**, *130*, 2730.
(7) Lin, R.; Taberna, P. L.; Chmiola, J.; Guay, D.; Gogotsi, Y.; Simon, P. *J. Electrochem. Soc.* **2009**, *156*, A7.
(8) Raymundo-Pinero, E.; Leroux, F.; Beguin, F. *Adv. Mater.* **2006**, *18*, 1877.
(9) Zhang, L. L.; Wei, T.; Wang, W.; Zhao, X. S. *Microporous Mesoporous Mater.* **2009**, *123*, 260.
(10) Wang, Y. G.; Li, H. Q.; Xia, Y. Y. *Adv. Mater.* **2006**, *18*, 2619.
(11) Wang, D. W.; Feng, L.; Liu, M.; Lu, G. Q.; Cheng, H. M. *Angew. Chem., Int. Ed.* **2008**, *47*, 373.
(12) Pandolfo, A. G.; Hollenkamp, A. F. *J. Power Sources* **2006**, *157*, 11.
(13) Salitra, G; Soffer, A; Eliad, L; Cohen, Y; Aurbach, D. *J. Electrochem. Soc.* **2000**, *147*, 2486.
(14) Long, J. W.; Dunn, B.; Rolison, D. R.; White, H. S. *Chem. Rev.* **2004**, *104*, 4463.
(15) Lee, K. T.; Lytle, J. C.; Ergang, N. S.; Oh, S. M.; Stein, A. *Adv. Funct. Mater.* **2005**, *15*, 547.
(16) Chai, G. S.; Shin, I. S.; Yu, J. S. *Adv. Mater.* **2004**, *16*, 2057.
(17) Woo, S. W.; Dokko, K.; Nakano, H.; Kanamura, K. *J. Mater. Chem.* **2008**, *18*, 1674.
(18) Liu, H. J.; Cui, W. J.; Jin, L. H.; Wang, C. X.; Xia, Y. Y. *J. Mater. Chem.* **2009**, *19*, 3661.

Published on Web 11/24/2009

storage capacity than the EDL capacitance. PANI, a conducting polymer, is a potential electrode material for pseudocapacitor applications because of its low cost, high conductivity in doped form, fast and stable transition between doped and reduced states, and easy synthesis using both chemical and electrochemical methods.[19−23] However, degradation due to the swelling and shrinkage during the charge−discharge process leads to poor cycle performance. Research has been done to increase the utilization of the electro-active material by supporting PANI on carbon-based materials.[10,24−29] The best electrochemical performance was observed on a PANI-porous carbon monolith composite electrode with a specific capacitance of 2200 F/g for the pure PANI phase.[29] The authors also found that the electrode performance is largely determined by the structure of the porous carbon monolith.

In our previous work, 3DOM carbon with microporous walls has been shown to be a good electrode material for electrochemical oxidation of methanol.[30] For electrode applications in supercapacitors, the macropores interconnected by openings of controllable size can greatly facilitate the transport of electrolyte ions, and the micropores may afford a nice environment for charge storage.[31] To improve the electrochemical performance, PANI was coated on the surface of 3DOM carbon in this work, aimed to fabricate PANI-3DOM carbon composite electrodes for applications in supercapacitors. Such composites embrace desirable electrode properties, such as chemical stability because of the carbon matrix, small mass transport resistance owning to the hierarchical porous structure, and pseudocapacitive properties due to the presence of active species PANI. Our experimental results indeed showed that a very high specific capacitance of as high as 1490 F/g was realized for PANI in the composite. Good rate performance and cycle ability were also observed over the composite electrode. The significantly enhanced electrochemical properties were found to be strongly related to the three-dimensionally interconnected hierarchical porous structure as well as the morphology of the active materials.

Scheme 1. Preparation Process of 3DOM Carbon and 3DOMC-PANI Composite

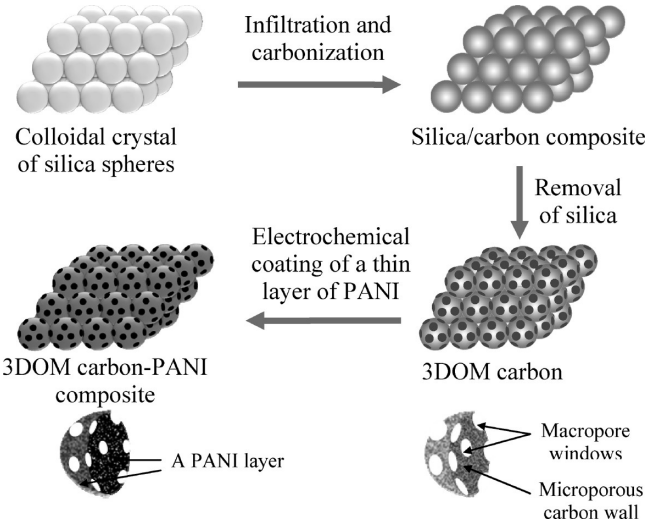

Experimental Section

Preparation of 3DOM Carbon. Scheme 1 illustrates the preparation procedure. Colloidal SiO_2 spheres with an average diameter of 550 nm synthesized using the Stöber method were assembled to form a colloidal crystal using the gravitational sedimentation method.[32] The colloidal crystal was soaked in a glucose solution (30 wt %) for 20 min. The glucose-filled colloidal crystal template was dried at 80 °C for 4 h, followed at 150 °C for 6 h. The above infiltration steps were repeated to ensure a complete filling of the void spaces between the silica spheres by glucose. The sample was carbonized in a tube furnace under N_2 flowing at 850 °C for 6 h. The silica spheres were removed using a HF solution (48 wt %) to leave behind a surface-tempated 3DOM carbon after washing and drying in air at 60 °C.

Preparation of 3DOMC-PANI Composites. A 3DOMC-PANI composite sample was prepared by electrochemical polymerization of aniline on the surface of 3DOM carbon using the potentialdynamic method in a one-compartment cell connected to an Autolab PGSTAT302N station. As the 3DOM carbon is a nonpowder material and it is monolithic in shape, it does not require any binder during the electrode preparation. A small piece of 3DOM carbon sample was sandwiched into a Pt net with the remaining part covered by Telfon tape to use as the working electrode. The cell was equipped with a Pt sheet and a saturated Ag/AgCl electrode as the counter and the reference electrodes, respectively. An electrolyte solution consisting of 1 M H_2SO_4 and 0.05 M aniline was used for electrochemical deposition of PANI on the surface of the 3DOM carbon. The working electrode was immersed into the electrolyte for 0.5 h to facilitate the diffusion of aniline monomers to both the outer and the inner surfaces of the 3DOM carbon. The deposition of PANI was conducted using the potential dynamic method in the potential range of −0.2 and 0.8 V. The amount of deposited PANI was varied by using the same deposition time (8×10^3 s) but different sweep rates (2, 5, and 50 mV/s), thus the sweep cycles were different. The samples thus prepared were then washed repeatedly with deionized water and dried in air at 60 °C for 2 h. The amount of electrodeposited PANI was estimated by the mass difference of the 3DOM carbon before

(19) Montilla, F.; Cotarelo, M. A.; Morallon, E. *J. Mater. Chem.* **2009**, *19*, 305.
(20) Choi, S. J.; Park, S. M. *J. Electrochem. Soc.* **2002**, *149*, E26.
(21) Ryu, K. S.; Kim, K. M.; Park, N. G.; Park, Y. J.; Chang, S. H. *J. Power Sources* **2002**, *103*, 305.
(22) Gupta, V.; Miura, N. *Electrochem. Solid-State Lett.* **2005**, *8*, A630.
(23) Lei, Z.; Zhang, H.; Ma, S.; Ke, Y.; Li, J.; Li, F. *Chem. Commun.* **2002**, *7*, 676.
(24) Zhang, H.; Cao, G.; Wang, Z.; Yang, Y.; Shi, Z.; Gu, Z. *Electrochem. Commun.* **2008**, *10*, 1056.
(25) Meng, C.; Liu, C.; Fan, S. *Electrochem. Commun.* **2009**, *11*, 186.
(26) Bleda-Martinez, M. J.; Peng, C.; Zhang, S.; Chen, G. Z.; Morallon, E.; Cazorla-Amoros, D. *J. Electrochem. Soc.* **2008**, *155*, A672.
(27) Wang, H.; Hao, Q.; Yang, X.; Lu, L.; Wang, X. *Electrochem. Commun.* **2009**, *11*, 1158.
(28) Woo, S. W.; Dokko, K.; Nakano, H; Kanamura, K. *J. Power Sources.* **2009**, *190*, 596.
(29) Fan, L. Z.; Hu, Y. S.; Maier, J.; Adelhelm, P.; Smarsly, B.; Antonietti, M. *Adv. Funct. Mater.* **2007**, *17*, 3083.
(30) Su, F.; Zhao, X. S.; Wang, Y.; Zeng, J.; Zhou, Z.; Lee, J. Y. *J. Phy. Chem. B.* **2005**, *109*, 20200.
(31) Chmiola, J.; Yushin, G.; Gogotsi, Y.; Portet, C.; Simon, P.; Taberna, P. L. *Science* **2006**, *313*, 1760.
(32) Stöber, W.; Fink, A.; Bohn, E. *J. Colloid Interface Sci.* **1968**, *26*, 62.

and after the deposition.[29] The obtained composites were denoted as 3DOMC-PANI-x, where x stands for the scan rate. For example, sample 3DOMC-PANI-2 was prepared using eight sweep cycles (the sweep rate was 2 mV/s and the time was 8×10^3 s), and sample 3DOMC-PANI-50 was prepared using 200 sweep cycles (the sweep rate was 50 mV/s and the time was 8×10^3 s). To investigate the morphology change of PANI with deposition time, another sample was prepared by doubling the deposition time (i.e., 1.6×10^4 s) at a sweep rate of 2 mV/s. This sample is named 3DOMC-PANI2-16.

Characterization. The microscopic feature of the samples was observed on a field-emission scanning electron microscope (FESEM) (JSM 6700F, JEOL Japan) operated at 10 kV and a transmission electron microscope (TEM) (JEM 2010, JEOL, Japan) operated at 200 kV. The pore structure of the sample was investigated using physical adsorption of nitrogen at the liquid-nitrogen temperature (77 K) on an automatic volumetric sorption analyzer (NOVA1100, Quantachrome). Prior to measurement, a sample was vacuum-degassed at 200 °C for 5 h. The specific surface area (S_{BET}) was determined according to the Brunauer−Emmett−Teller (BET) method in the relative pressure range of 0.01 − 0.2. The total pore volume (V_t) was obtained from the volume of nitrogen adsorbed at a relative pressure of 0.99. The microporosity was estimated using the t-plot method. The pore size distribution (PSD) curve was calculated using the density functional theory (DFT) method from the adsorption branch. X-ray photoelectron spectroscopy (XPS) analysis was carried out on an AXIS HSI 165 spectrometer (Kratos Analytical) using a monochromatized Al Kα X-ray source (1486.71 eV).

Electrochemical Evaluation. A three-electrode cell system was used to evaluate the electrochemical performance by both cyclic voltammetry (CV) and galvanostatic charge−discharge techniques on an Autolab PGSTAT302N at room temperature. A 2 M H_2SO_4 aqueous solution was employed as the electrolyte. The working electrode was prepared by fixing the carbon or the composite materials on Pt net. A platinum sheet and a saturated Ag/AgCl electrode were used as the counter and the reference electrodes, respectively. The specific gravimetric capacitance (C_{tot} in F/g) was obtained from the discharge process according to the following equation:

$$C_{tot} = \frac{I\Delta t}{\Delta V \times m} \quad (1)$$

where I is the current loaded (A), Δt is the discharge time (s), ΔV is the potential change during discharge process, and m is the mass of active material in a single electrode (g).

Results and Discussion

Preparation and Characterization of Materials. The colloidal crystal of close-packed monodisperse silica spheres was used as template for the preparation of 3DOM carbon. The structure of the colloidal crystal template and its inverse carbon structure are shown in Figure 1. The pore size of the 3DOM carbon depends on the size of the silica spheres forming the colloidal crystal template.[17] The intersphere interface induced by the sintering process ensured the removal of silica during the HF etching process. However, too much sintering may result in closing the passages between the octahedral and tetrahedral voids in the original colloidal crystal lattice.[33] The well-ordered colloidal structure with close-packed monodisperse silica spheres are clearly seen in Figure 1a. Using the colloidal crystal as a template, an inverse carbon structure was obtained as is seen in Figure 1b. The 3DOM carbon possessed uniform periodic macropores with a diameter similar to that of the silica spheres packed in the colloidal crystal template. A three-dimensionally interconnected porous network with pore windows of about 100 nm in diameter was obtained after removing the silica template. No obvious structural shrinkage was observed on the 3DOM carbon sample. From the higher-magnification image depicted in Figure 1c, it appears that the pore wall of the 3DOM carbon is smooth. The TEM image shown in Figure 1d revealed a disordered microporous texture of the macropore wall. The presence of micropores is ascribed to the emission of small gaseous molecules (e.g., CO_2, H_2, and H_2O) during the carbonization process.

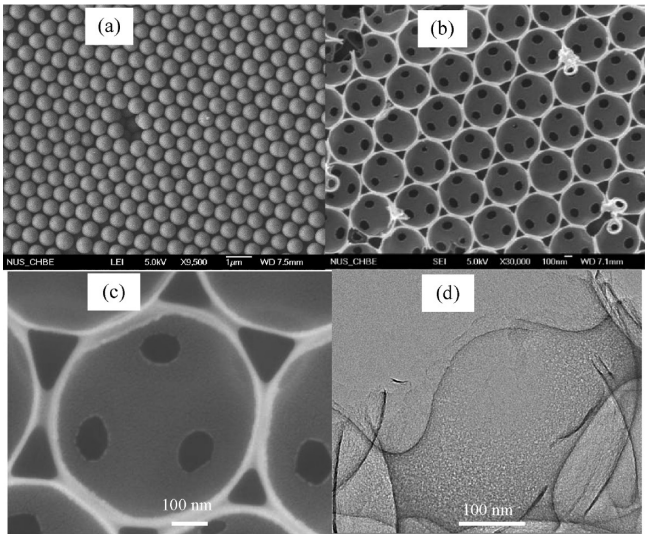

Figure 1. FESEM images of self-assembled colloidal crystal template (a), inverse 3DOM carbon (b, c), and TEM image of the 3DOM carbon (d).

The nitrogen adsorption−desorption isotherms are shown in Figure 2a. The isotherms are characteristic of a combination of type I and type II isotherms. The type I isotherm is featured by prominent adsorption below the relative pressure of $P/P_0 = 0.1$, which is due to the micopore filling or monolayer adsorption due to strong adsorbent−adsorbate interactions.[34] At the high relative pressure region ($P/P_0 > 0.9$), the isotherm is characteristic of multilayer adsorption on a macroporous solid.[15] The adsorption-branch pore size distribution curve computed using the DFT method is shown in Figure 2b. It is seen that the sample has micropores with an average pore diameter of about 1.4 nm. The BET specific surface area and total pore volume were calculated to be 1164 m^2/g and 0.86 cm^3/g, respectively. The micropore surface area estimated using the t-plot method was about 709 m^2/g. From the FESEM, TEM, and the nitrogen sorption

(33) Zakhidov, A. A.; Baughman, R. H.; Iqbal, Z.; Cui, C.; Khayrullin, I.; Dantas, S. O. *Science*. **1998**, *282*, 897.

(34) Kruk, M.; Jaroniec, M. *Chem. Mater*. **2001**, *13*, 3169.

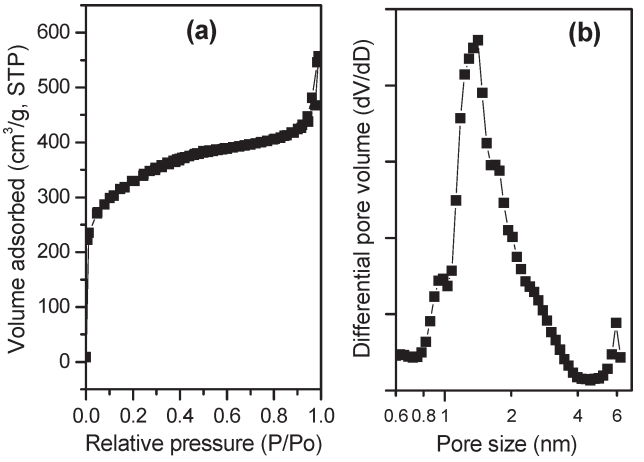

Figure 2. Nitrogen adsorption−desorption isotherm (a) and adsorption-branch PSD curve (b) of the 3DOM carbon material.

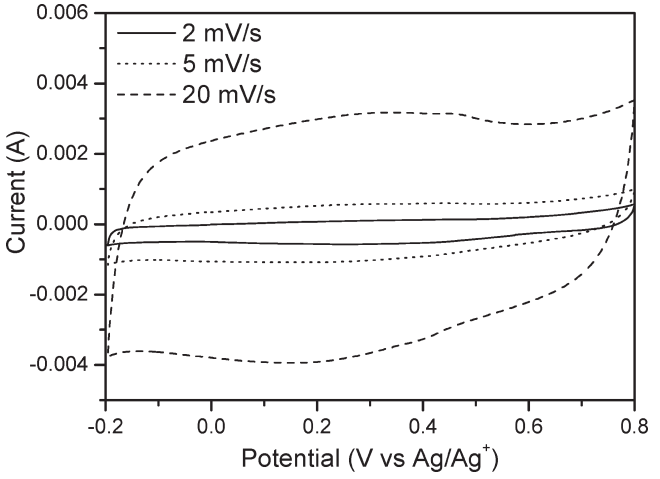

Figure 3. CV curves of 3DOM carbon in 2 M H_2SO_4 at different scan rates.

results, it can be concluded that the 3DOM carbon has a bimodal porous structure with micropores on the macropore walls. Such a porous structure is favorable in electrochemical energy storage because the interconnected macropores ensure the electrolyte transport through the material. The micropores on the pore wall can shorten the diffusion length and are efficient in accumulation of charges.[11,18,35]

CV and charge−discharge measurements were conducted to assess the performance of 3DOM carbon as supercapacitors electrode in acidic electrolyte. The CV curves shown in Figure 3 retained rectangular shapes at all sweep rates. The steep slope in the current change at the switching potentials indicates a small mass-transfer resistance. The capacitances calculated from the galvanostatic charge−discharge data were 140 and 125 F/g at the current loadings of 0.5 and 1 A/g, respectively. The above electrochemical results demonstrate that the 3DOM structure possesses a good rate performance, but a poor energy density.

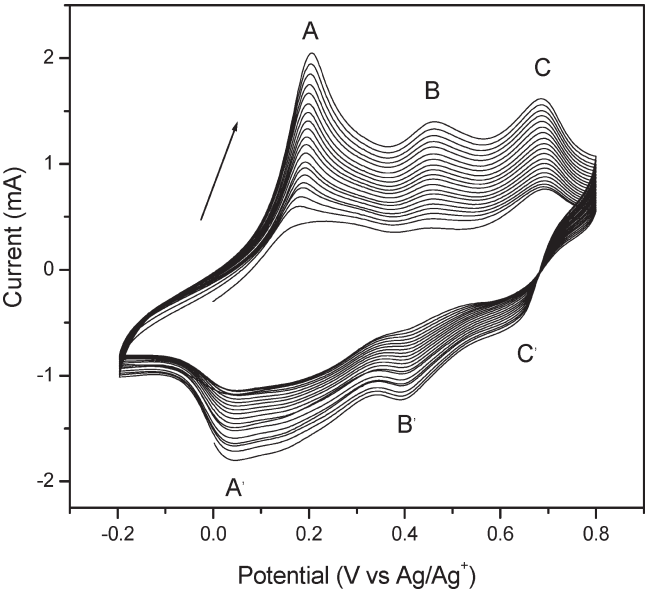

Figure 4. CV curves showing the growth of PANI on 3DOM carbon in 1 M H_2SO_4 with 0.05 M aniline between the potential range of −0.2 and 0.8 V at a sweep rate of 5 mV/s.

Physical and Chemical Properties of 3DOMC-PANI Composites. Electrochemical polymerization of aniline monomer on 3DOM carbon was conducted in 1 M H_2SO_4 with 0.05 M aniline using the potentialdynamic method. Various sweep rates and different deposition times were used to achieve different loading amounts and morphologies of the deposited PANI. The cyclic voltammograms recorded at 5 mV/s between the potential range of −0.2 and 0.8 V are shown in Figure 4. Three pairs of redox peaks labeled as A/A', B/B', to C/C', corresponding to the different processes of the PANI redox transitions can be seen. The two pairs of peaks A/A' and C/C' are associated with the redox of PANI molecules (leucoemeraldine and perigraldine species).[36] The weak peaks B/B' are attributed to the double-electron redox transition between *p*-benzoquinone and the *p*-hydroquinone through hydrolysis reaction of PANI.[37−39] It is known that the hydrolysis peaks appear when PANI is oxidized at potential higher than 0.7 V (vs saturated calomel electrode) and the degradation products of PANI with shorter chains are produced.[26] The gradual increase in the current with the number of cycles indicated the growth of PANI. The loading of PANI ranging from 8 to 35 wt % was controlled by the electrodeposition parameters (sweep rate and number of cycles) in the present study.

The intrinsic oxidation state of PANI ranges from the fully oxidized pernigraniline ($n = 0$, $m = 1$), through half-oxidized emeraldine ($n = m = 0.5$), to fully reduced leucoemeraldine ($n = 1$, $m = 0$).[20,36,40] The basic chemical structure of PANI molecule is shown in Scheme 2. Since

(35) Hu, Y. S.; Adelhelm, P.; Smarsly, B. M.; Hore, S.; Antonietti, M.; Maier, J. *Adv. Funct. Mater.* **2007**, *17*, 1873.
(36) Lee, Y.; Chang, C.; Yau, S.; Fan, L.; Yang, Y.; Yang, L. O. *J. Am. Chem. Soc.* **2009**, *131*, 6468.
(37) Spataru, T.; Spataru, N.; Fujishima, A. *Talanta.* **2007**, *73*, 404.
(38) Hand, R. L.; Nelson, R. F. *J. Am. Chem. Soc.* **1974**, *96*, 850.
(39) Stilwell, D. E.; Park, S. M. *J. Electrochem. Soc.* **1988**, *135*, 2254.
(40) Golczak, S.; Kanciurzewska, A.; Fahlman, M.; Langer, K.; Langer, J. *J. Solid State Ionics.* **2008**, *179*, 2234.

Scheme 2. Structure of PANI ($n + m = 1$)

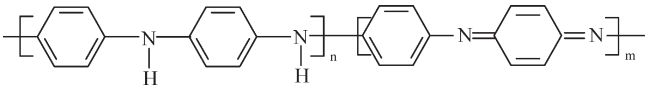

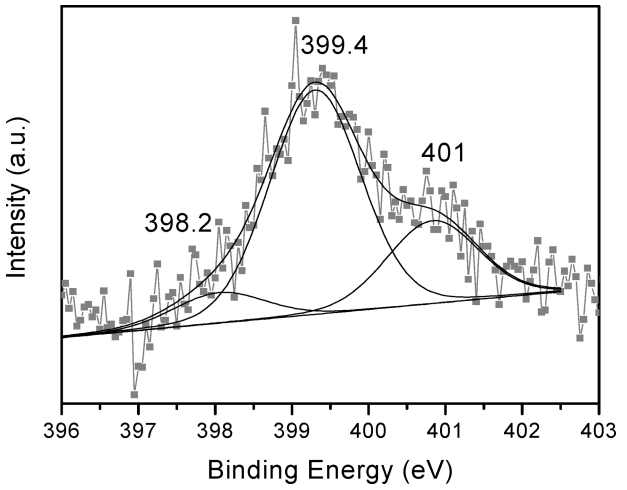

Figure 5. N 1s XPS core-level spectra of the composite 3DOMC-PANI-5.

the chemical and electrical properties of PANI are closely linked to its intrinsic structure, which is the distribution of quinonoid imine (—N═), benzenoid amine (—NH—) as well as the positively charged nitrogen, XPS analysis was employed to identify the chemical nature of the PANI formed on the 3DOM carbon. As seen in Figure 5, the deconvolution of N 1s core-level spectra resulted in three peaks: the benzenoid amine centered at 399.4 eV, the quinonoid imine at 398.2 eV, and the nitrogen cationic radical (N^+) at 401 eV.[36,40] The last peak is indicative of the doping level of the polymer.[41] Based on the quantitative analysis of the deconvoluted N1s spectra, a N^+/N ratio of 0.25 was obtained, indicating a high proton doping for the deposited PANI thin film. The doping level is a very important factor affecting the electrical and other properties of PANI. A high doping level affords a better electronic conductivity,[39−41] which is desirable in many applications, particularly in electrochemical applications.

Figure 6 shows the FESEM and TEM images of the 3DOMC-PANI composites with different loadings of PANI. Compared to the pure 3DOM carbon, the morphology changed slightly for the composites. Thin layer of PANI with different thicknesses were deposited on both inner and outer surfaces of 3DOM carbon as seen in Figure 6a−c. This is desirable because both surfaces containing thin layer of PANI are effective in contributing pseudocapacitance to the total energy storage. It is also seen that with the increase in the loading of PANI, the pore window size became smaller and smaller. The low-magnification TEM image shown in Figure 6e showed no obvious change comparing to the pure 3DOM carbon, indicating the deposited PANI layer is

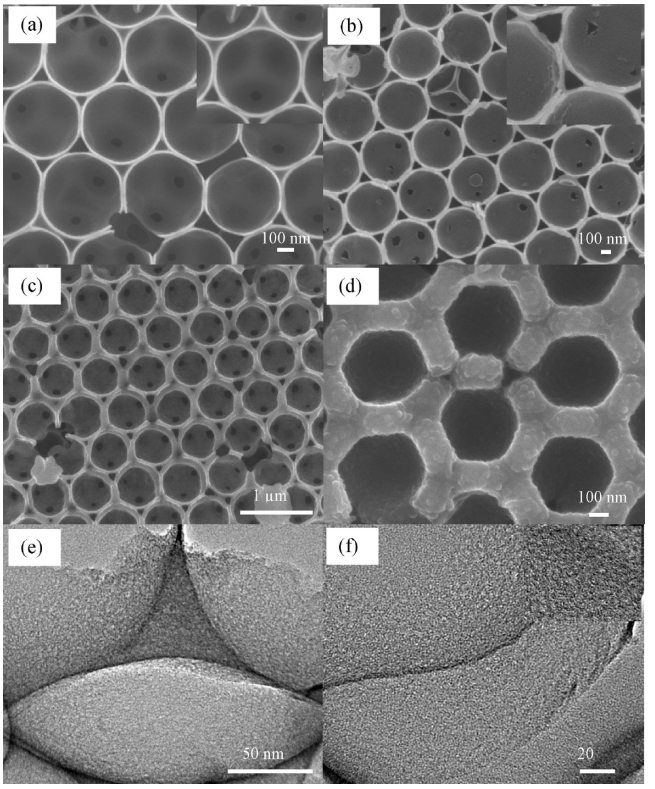

Figure 6. FESEM images of 3DOMC-PANI-2 (a), 3DOMC-PANI-5 (b), 3DOMC-PANI-50 (c), 3DOMC-PANI2−16 (d); TEM images of 3DOMC-PANI-5 at different magnifications (e and f).

thin. The thin layer of PANI can be seen on the macroporous carbon wall by careful examination of the TEM image in Figure 6f. The high-magnification TEM image (inset in Figure 6f) indicated that the wall of the composite consists of disordered micropores, implying that the PANI layer is not only thin but also porous. In contrast, a thick layer of PANI is observed in Figure 6d when the electrodeposition time was doubled at the sweep rate of 2 mV/s. Most of the pore windows are closed with the deposition of thick layer of PANI. The morphology of the PANI is very important because the pseudocapacitive properties depend very much on the surface utilization of the active materials.[10,42] On the other hand, the closure of the pore windows will inevitably cause the blockage of the interconnected three-dimensional network, which will affect the electrolyte transportation. Hence, a thin and porous layer with short ionic diffusion path is advantageous in electrochemical application.

Electrochemical Properties of 3DOMC-PANI Composites. CV and charge−discharge testes were employed to characterize the electrochemical performance of various 3DOMC-PANI composites. Figure 7a compares the CV curve of a pure 3DOM carbon with composites 3DOM-PANI-50 (18 wt % PANI), 3DOM-PANI-5 (11 wt %) and 3DOM-PANI-2 (8 wt % PANI) at the scan rate of 5 mV/s. In contrast to the pure 3DOM carbon with a rectangular shape of CV, the composites displayed distinct redox peaks, which were attributed to the

(41) Hu, C. C.; Lin, J. Y. *Electrochim. Acta* **2002**, *47*, 4055.

(42) Zhang, H.; Li, H.; Zhang, F.; Wang, J.; Wang, Z.; Wang, S. *J. Mater. Res.* **2008**, *23*, 2326.

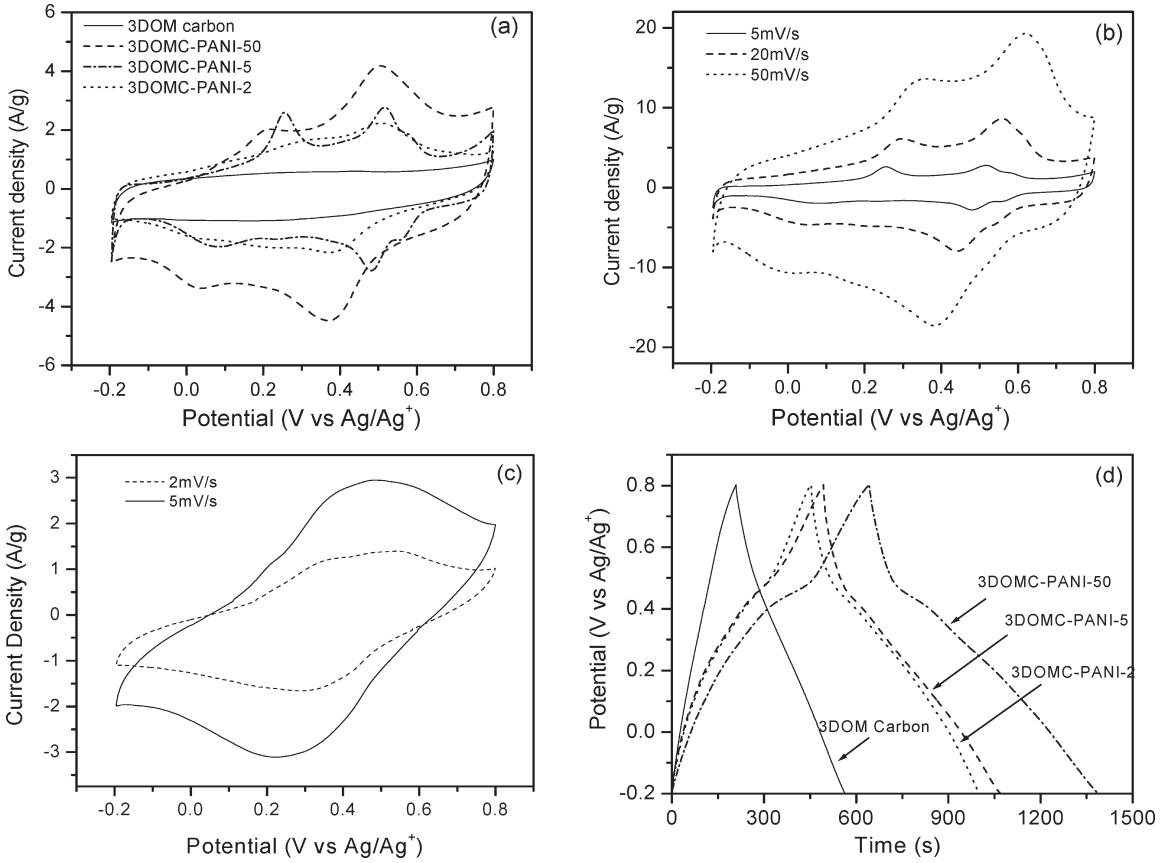

Figure 7. CV comparison of 3DOM carbon with its composites 3DOMC-PANI at the scan rate of 5 mV/s (a); CV plots at different scan rates for 3DOMC-PANI-5 (b) and 3DOMC-PANI2−16 (c); Charge−discharge performance of 3DOMcarbon and its composites (d).

pseudocapacitive properties of the deposited PANI layer. Two pairs of peaks can be seen: the first oxidation peak at around 0.25 V is related to the transition of PANI from its semiconducting-state (leucoemeraldine form) to a conducting state (polaronic emeraldine form). The second peak is due to the emeraldine-pernigranline transition.[10,19] The corresponding counter processes can be observed during the reverse scan. For the composite materials with a thin layer of PANI, the redox current was found to increase with the amount of coated PANI. It is observed in Figure 7b that there is a slight positive shift of the oxidation peaks with an increase in the sweep rates. This is mainly due to a slight increase in the series resistance over porous electrodes at high sweep rates.[10] In addition, as shown in Figure 7b, the steep slopes at the switching potentials retained after the deposition of PANI at various scan rates, indicating well preserved three-dimensionally interconnected porous network with thin layer of PANI on both inner and outer carbon surfaces.

When a thicker layer of PANI was deposited with prolonged deposition time (sample 3DOMC-PANI2-16), a large resistance was observed as evidenced by the tilted CV curves shown in Figure 7c. This is probably due to the partial blockage of the interconnected pores by the deposited PANI, which resulted in a slow transport of the electrolyte ions to the active species. Therefore, besides the chemical and electrical properties, the morphology of the deposited PANI also plays an important role in the overall electrochemical performance of the composite materials. A careful control over the deposited PANI can improve the capacitive performance of the electrode.

The largely improved capacitance performance after the incorporation of a thin layer of PANI can be clearly seen from the charge−discharge plot shown in Figure 7d. At the current density of 0.5 A/g, the specific capacitance was enhanced from 140 F/g for pure 3DOM carbon to 352 F/g for composite 3DOMC-PANI-50. With the effective pseudocontribution of PANI deposited on both the inner and outer surfaces of 3DOM carbon, better capacitive performance was observed in comparison to the composite electrode with only inner PANI deposition.[28]

Table 1 summarizes the capacitive performance of all electrode materials. It can be observed over 2.5 times increase in capacitance was achieved by electrodeposition of a thin layer of PANI on the macroporous carbon surface with little rate deterioration. However, it can be clearly seen that the rate retention was decreased when thick layer of PANI was deposited. This is in line with the above conclusion that the excess PANI deposition would block the pore window which may slow down the mass transport of electrolyte ion.

To find out the pseudocapacitive contribution from the PANI, the specific capacitance of pure PANI in the composite was calculated by subtracting the double-layer capacitance from the overall capacitance of the composite electrode. It can be seen from Table 1 that the highest

Table 1. EC Performance of Various Electrode Materials[a]

samples	current density (0.5 A/g)			current density (1 A/g)		
	PANI (wt%)	C_{tot} (F/g)	C_{PANI} (F/g)	C_{tot} (F/g)	C_{PANI} (F/g)	rate retention (%)
3DOM carbon	0	140		125		83.9
3DOMC-PANI-50	18	352	1318	278	975	79.0
3DOMC-PANI-5	11	287	1476	243	1198	84.7
3DOMC-PANI-2	8	248	1490	220	1313	88.7
3DOMC-PANI2−16	35	259	480	187	302	72.2

[a] C_{tot} is the total specific capacitance of the composite. [b] C_{PANI} is the specific capacitance of PANI in the composite.

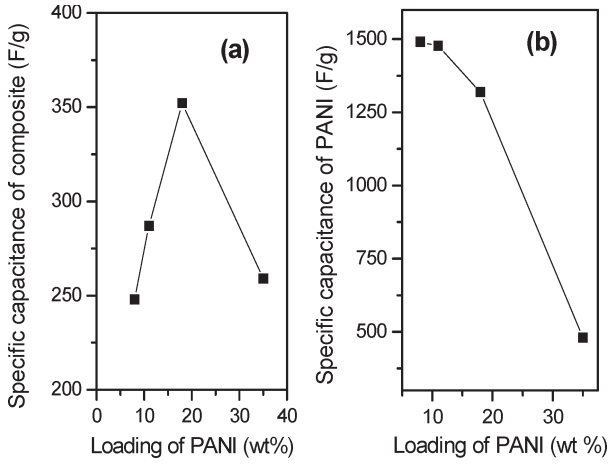

Figure 8. Specific capacitance of the composite materials (a) and specific capacitance of PANI in the composite (b) vs the mass loading of PANI at current density of 0.5 A/g.

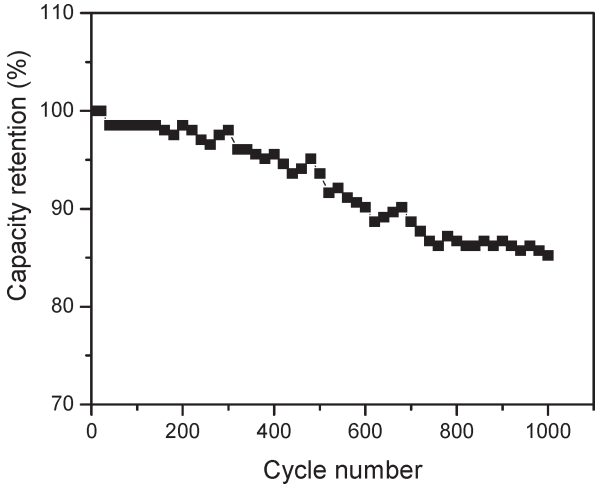

Figure 9. Cycling performance of composite 3DOMC-PANI-5 under a current density of 1.5 A/g.

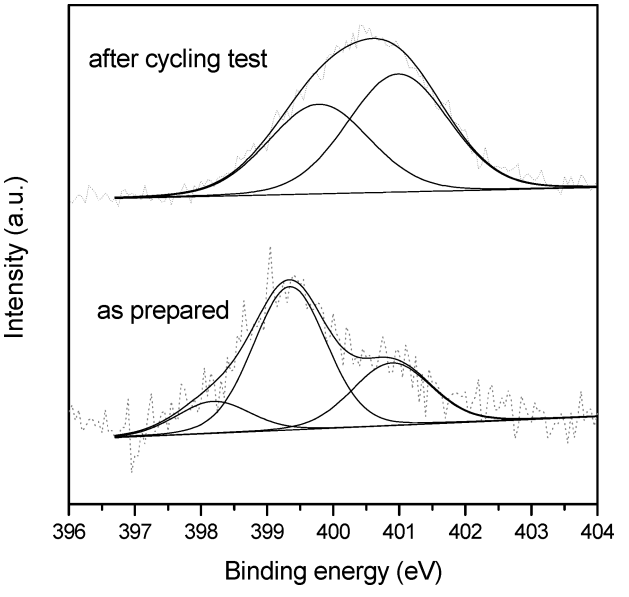

Figure 10. N 1s XPS core-level spectra of the composite 3DOMC-PANI-5 before and after cycling test.

capacitance of PANI was estimated to be about 1490 F/g at the current density of 0.5 A/g for electrode 3DOMC-PANI-2. The value was slightly reduced to 1313 F/g when the current density was increased to 1 A/g. The capacitance performance of the composite materials with different loadings of PANI is shown in Figure 8. The total capacitance of the composite was increased with the increase in the amount of PANI deposited, then decreased when a thicker PANI layer was formed. It is also noted that the pseudocapacitance of PANI in the composite with a thin PANI layer all exceeded 1300 F/g. However, for the composite with a thick layer of PANI (sample 3DOMC-PANI2-16), the pseudocapacitance of PANI was only about 480 F/g, demonstrating that the pseudocapacitive contribution from the active material is mainly due to the fast faradic reaction at the electrode surface. The effective utilization of the active species is crucial in the realization of pseudocapacitance. In addition, the three-dimensionally interconnected porous structure is very important to ensure the fast transport of electrolyte ions to the active surface. Hence, a thin and porous layer of active material with a short ionic diffusion path is favorable for electrochemical energy storage.

The advantages of the 3DOMC-PANI composite electrode materials lie in the combination of the essential properties of the hierarchical porous carbon and the PANI thin layer. With a power density of 3 kW/kg, the specific energy density was estimated to be about 182 Wh/kg based on the pure PANI phase in a single electrode. An overall capacitance of 352 F/g was obtained for the composite electrode at a current density of 0.5 A/g, which corresponds to a specific energy density of 49 Wh/kg. This capacitive performance of the composite electrode is much better than some commercial activated carbons, whose specific capacitances are lower than 200 F/g.[3] In addition, Fan and co-workers have pointed out that the electrode performance is greatly affected by the porosity and interconnected porous structure.[29] Hence,

3DOMC-PANI composite materials which offer good pore control with well ordered three-dimensionally interconnected porous network are desirable as supercapacitor electrodes.

Figure 9 shows the electrochemical stability of composite electrode 3DOMC-PANI-5 at a current density of 1.5 A/g. It is seen that over 85% of the original capacitance was retained after 1000 cycles, indicating a good cycle ability of the composite materials. Attempts were made to study the chemical composition of PANI phase during the electrochemical test by conducting XPS analysis on the composite sample 3DOMC-PANI-5 before and after the cycling test. Figure 10 showed the deconvolution of N 1s core-level spectra before and after the cycling test. Two main peaks were observed on the sample after the cycling test, which are benzenoid amine (—NH—) and nitrogen cationic radical (N^+). The relative intensity of these two peaks is almost identical, which implies that it is essentially half-oxidized emeraldine form of PANI.[36] Compared to the as-prepared composite sample, the changes in the chemical composition of PANI phase suggested the modification of active species by protonation process during the cycling test. This is evidenced by the largely increased doping level after the cycling test.

Conclusions

In summary, we have demonstrated the preparation of polymer-carbon composite electrode materials consisting of hierarchical 3DOM carbon and a thin layer of PANI. The composite combines the essential properties of the carbon substrate and the pseudoactive species of PANI. The electrochemical results showed that the composite electrode possessed good capacitive properties and a very high specific capacitance (1490 F/g) for PANI in the composite. The performance of the composite strongly depended on its microtexture. The advantages of using hierarchical 3DOM carbon as a support for PANI are summarized as follows: (1) the ordered three-dimensionally interconnected macroporous structure provides a fast ion transportation pathway for the electrolyte to reach the surface of the active material; (2) it serves as a good support to overcome the degradation problem during cycling; (3) it provides a large surface for the deposition of active materials, thus increasing the utilization of the electroactive regions; (4) it contributes EDL capacitance to the overall energy storage. Additionally, a thin and porous layer of PANI deposited on the carbon wall can greatly shorten the diffusion length, hence providing not only an enhanced energy storage capacity but also a good rate capability. The greatly enhanced electrochemical properties of the composite materials are attributed to their designed chemical and physical properties.

Acknowledgment. Financial support from Ministry of Education Tier 2 Grant (Project No. MOE2008-T2-1-004) is acknowledged.